bid for 4 days). Groups were compared by analysis of variance (ANOVA) using the nonparametric Kruskall–Wallis test. $*P < 0.05$ as compared to PBS. $^{\#}P < 0.05$ as compared to Gleevec. $P < 0.05$ as compared to FL.

Gleevec acts on host DCs to promote NK cell activation. Since a subset of mature NK cells expresses KIT and exhibits higher cytotoxic activity than the KIT^- NK cell subpopulation (13), we investigated the direct effect of Gleevec on NK cells. In vivo treatment with FL+Gleevec did not augment the frequency of KIT^+ NK cells (7% ± 2% of total NK cells in FL+Gleevec versus 7.2% ± 2.6% in controls). Furthermore, Gleevec could not directly boost IFN-γ production by bulk NK cells in vitro (Figure 4A). Since FL is known to amplify DCs, (14) and since mature DCs have the unique capacity to promote NK cell effector functions including IFN-γ secretion and antitumor effects in vivo (10, 15), we hypothesized that Gleevec could confer an NK cell stimulatory capacity to host DCs. Gleevec enhanced IFN-γ production by NK cells, but only when NK cells were cocultured with mouse bone marrow–derived DCs (BM-DCs) (Figure 4A) or spleen-derived DCs (data not shown) stimulated with 10 nM to 1 μM of Gleevec for 20 hours. In untreated controls, one BM-DC triggered only 2 NK cells, whereas one Gleevec-pretreated BM-DC ($BM\text{-}DC^{STI}$) efficiently triggered 10 NK cells (Figure 4B). Tyrphostin AG957, a nonselective tyrosine kinase inhibitor (16), did not promote DC-mediated NK cell activation (Figure 4B). Adoptive transfer of $BM\text{-}DC^{STI}$ into $Swiss^{nu/nu}$ mice led to NK cell activation, as indicated by the upregulation of CD69 on splenic $DX5^+/CD3^-$ NK cells (data not shown). IL-2, IL-12, and IL-18 were not detectable in the supernatants of BM-DCs cultured alone or cocultured with NK cells, whether stimulated with Gleevec or not. Since Gleevec-mediated NK cell activation was also observed in IL-12 $p35^{-/-}$ BM-DCs, we ruled out a role for IL-12 (Figure 4C). The levels of thymus and activation-regulated chemokine (TARC), macrophage-derived chemokine (MDC), and fractalkine were similar in BM-DCs and Gleevec-treated BM-DCs, whether they were cultured alone or cocultured with NK cells (data not shown). We confirmed that the NK cell stimulatory activity was not contained in the supernatants of Gleevec-stimulated BM-DCs, but rather was associated with the DC membrane since separation of Gleevec-pretreated BM-DCs from NK cells significantly hampered NK cell activation by DCs (Figure 4D).

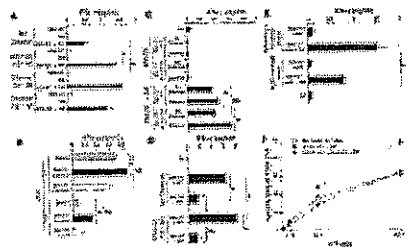

View larger version (26K):

[in this window]

[in a new window]

Figure 4

Gleevec endowed DCs with NK cell stimulatory capacity. (A) Mouse DCs pretreated with Gleevec exhibited enhanced NK cell stimulatory capacity in vitro. BM-DC+NK coculture supernatants were monitored for IFN-γ secretion. Gleevec alone or FL+Gleevec did not trigger NK cell cytotoxicity or IFN-γ production in the absence of BM-DCs. (B) Gleevec but not tyrphostin (AG957) enhanced the NK stimulatory activity of DCs. Experiments were conducted in triplicate at various DC/NK ratios (1:2, 1:10) in the presence of Gleevec or tyrphostin. (C) IL-12 is not involved in the Gleevec-mediated NK cell activation. Conventions as in A but using IL-12p35 loss-of-function BM-DCs instead of WT BM-DCs. (D) STI-mediated NK cell activation depends on cell-cell contact. BM-DC and NK cell cocultures were separated or not by a trans-well membrane (BM-DC // NK). (E) Long-term exposure to Gleevec enhanced the host $CD11c^+$ DC capacity to activate NK cells. Cell-sorted $CD11c^+$ $B220^-$ splenocytes from C57BL/6 mice treated either with H_2O or Gleevec for 15-21 days were incubated for 20 hours with NK cells as in A. IFN-γ release was measured. One representative experiment (out of 2) is shown. (F) Human $CD34^+$-derived DCs stimulated with Gleevec also promoted NK cell activation. After coculture of $CD34^+$-derived DCs with purified human NK cells, NK cell cytolytic activity was observed against K562. Means of triplicate wells are represented (standard errors were consistently less than 10% of means). One representative experiment (out of 5) is depicted. Groups were compared by ANOVA using the nonparametric Kruskall-Wallis test ($*P < 0.05$).

To confirm that DCs were among the pharmacological targets of Gleevec in vivo, we purified splenic $CD11c^+$ DCs from Gleevec-treated mice and cultured them with NK cells. Long-term treatment with Gleevec markedly enhanced the NK cell stimulatory capacities of splenic $CD11c^+$ DCs (Figure 4E). We also investigated the role of Gleevec in the differentiation and activation of $CD11c^+$ DCs in nude mice treated with FL. FL was administered on a daily basis for 10 days, and Gleevec was given orally from day 7 to day 10. Spleens were harvested at day 13, allowing enumeration of $CD11c^+/CD11b^-$ and $CD11c^+/CD11b^+$ DC subsets in flow cytometry. As shown in Table 1,

there were significantly more DCs in mice that received the combination of FL and Gleevec than in littermates receiving FL alone. Both DC subsets — $CD11c^+/CD11b^-$ and $CD11c^+/CD11b^+$ — were increased after therapy with FL combined with Gleevec. However, the levels of MHC class II and costimulatory molecules were comparable in both groups, suggesting that Gleevec did not promote DC maturation in vivo and that the NK cell activation observed in vivo was not triggered by the maturation of $CD11c^+$ DCs in mice. Gleevec also triggered DC-mediated NK cell activation in the human system as measured by the enhanced lysis of K562 cells by $CD56^+/CD3^-$ peripheral blood NK cells cocultured with human DCs derived from $CD34^+$ precursors and pretreated with Gleevec (Figure 4F). Importantly, Gleevec did not trigger DC maturation in vitro, as assessed by FACS analysis and mixed T lymphocyte reactions (Supplemental Figure 2). Thus, Gleevec selectively promoted the capacity of DCs to stimulate NK cells, but not T cells.. Thus, Gleevec alone or combined with FL promoted NK cell activation in vivo, leading to NK cell-dependent antitumor effects. Host DCs were pharmacological targets of Gleevec and acquired NK cell stimulatory capacity in vitro and in vivo.

View this table: [in this window] [in a new window]

Table 1

The combination of FL and Gleevec enhanced differentiation or survival of CD11c+ DC in vivo

KIT signaling in DCs inhibits NK cell activation. We next addressed the involvement of the KIT-dependent transduction pathway in the DC-mediated NK cell activation promoted by Gleevec. Indeed, KIT is expressed on BM-DCs from day 4 to day 6 of the in vitro culture in GM-CSF and IL-4, as well as on $CD11c^+$ DCs in vivo (Supplemental Figure 3, A and B). Therefore, we compared the NK cell functions of KIT-deficient (WBB6F1 Kit^W/Kit^{W-v}; W/Wv) mice with those of wild-type $WBB6F1^{+/+}$ (WT) control mice following stimulation with BM-DCs in vitro or with FL+Gleevec in vivo. The W-v mutant receptor exhibits a point mutation at position 660 of the c-kit sequence (17, 18), thereby reducing its kinase activity to roughly 10% of wild-type levels. BM-DCs from W/Wv mice displayed the typical phenotypic profile of fully differentiated BM-DCs (Supplemental Figure 4), but were more efficient than WT BM-DCs in activating allogeneic NK cells, but not T cells (not shown) with regard to their ability to trigger NK cell lysis of YAC-1 (Figure 5A) and IFN-γ production (Figure 5B). Importantly, Gleevec failed to further enhance the capacity of W/Wv BM-DCs to promote NK cell activation (Figure 5), which is in line with the fact that the pharmacological target of Gleevec was already inhibited. In vivo administration of FL alone (without Gleevec) was able to trigger upregulation of CD69 on W/Wv NK cells (and IFN-γ secretion in splenocytes stimulated ex vivo with IL-2; not shown), while the combination of both FL and Gleevec was required to activate NK

cells in WT control mice (Figure 5C). This further supports the notion that Gleevec has to act on KIT to induce the DC-mediated NK cell activation. In other words, the treatment with Gleevec provides a phenocopy of the W/Wv mutation. Of note, the enhanced NK cell activity observed in W/Wv mice following administration of FL could not be accounted for by the absolute numbers of NK cells or by the mutation itself. Indeed, FL did not augment the absolute numbers of NK cells in W/Wv mice ($6.8 \pm 0.4 \times 10^6$ in WT versus $5.6 \pm 1.3 \times 10^6$ in W/Wv) as expected from previous reports (13). Moreover, the NK cell activity of c-kit$^{-/-}$ NK cells from NK-deficient mice (RAG2/$\gamma c^{-/-}$) reconstituted with fetal liver hematopoietic stem cells of W/Wv mice was poorly cytolytic (13). All these data indicate that Gleevec stimulates DC-mediated NK cell activity via a direct action on KIT expressed in DCs.

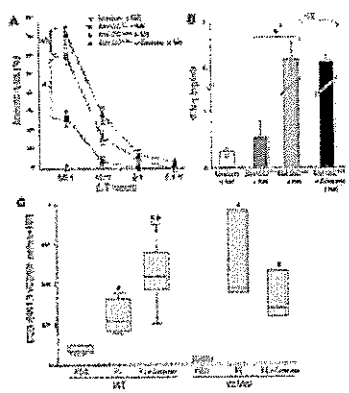

View larger version (23K):

[in this window]

[in a new window]

Figure 5

The c-kit loss-of-function mutation W/Wv conferred a phenotype similar, with regard to DC-mediated NK cell activation, to that found with Gleevec treatment. (A) Deficient KIT signaling enhanced the capacity of DCs to stimulate the cytotoxic activity of NK cells in vitro. The experimental setting was identical to that represented in Figure 4A, except that BM-DCs derived from WT WBB6F1 mice (WT) or from c-kit-deficient WBB6F1 mice (W/Wv) were cocultured with WT NK cells and NK cytotoxicity was assessed on YAC-1 cells (12). (B) Deficient KIT signaling stimulated the capacity of DCs to elicit IFN-γ secretion by NK cells in vitro. Instead of measuring the cytotoxic activity as in A, the accumulation of IFN-γ in culture supernatants was assessed. (C) The W/Wv mutation allowed FL-mediated NK cell activation in vivo. WT and W/Wv mutant mice were treated with FL in vivo (same doses, schedule, and statistical methods as in Figure 3). All experiments were performed 3 times with similar results. $^{\#}P < 0.05$, significantly different from PBS-treated animals (in W/Wv and WT animals); $^{*}P < 0.05$, significantly different from FL-treated animals.

NK cell activation in GIST patients treated with Gleevec. Intrigued by these findings, we wondered whether Gleevec might mediate part of its therapeutic effects on GIST patients through NK cells. To test this hypothesis, we assessed NK cell functions in 49 GIST patients, a fraction of whom were receiving oral therapy with Gleevec (Supplemental Table 1B). To evaluate the NK cell-activation status, we took advantage of an assay in which activated NK cells cocultured with immature allogeneic DCs in the presence of LPS produce IFN-γ (15, 19). In

these conditions, IFN-γ was produced in the circulating $CD3^-/CD56^+$ NK cells from 24 out of 49 (49%) GIST patients treated with Gleevec. In contrast, only 21% of untreated GIST or 11% of normal volunteers manifested signs of activation (Figure 6A). Of note, a longitudinal study revealed that Gleevec increased NK cell activation when data before and after treatment were compared in 9 out of 11 patients (Figure 6A, linked spots). More importantly, Gleevec-mediated NK cell activation correlated with clinical outcome. None of the patients who displayed enhanced NK cell functions exhibited progressive disease, while all 10 patients with Gleevec refractory GIST continued to manifest poor NK cell activity ($P < 0.05$, Figure 6B). We next studied the time to progression for 43 patients who benefited from a median follow-up of 13.2 months in both cohorts of GIST patients — those who exhibited enhanced NK cell function (22 out of 43) after 2 months of Gleevec and those who did not (21 out of 43). As shown in Figure 6C, the time to progression was significantly longer in patients with NK cell activation (log rank test, $P = 0.03$). Although prognostic factors influencing the response to Gleevec have not been clearly identified, four factors associated with poor prognosis were recently reported (20): extra-gastric primary tumor(s); a hemoglobin level of less than 7 g/dl; performance status over 2; and pulmonary metastases at entry. No significant differences were observed between the two cohorts (Gleevec-responsive versus Gleevec-unnresponsive NK cells) for any of the 4 parameters (69% vs. 75%, $P = 0.56$; 12.7 vs. 12.9 g/dl, $P = 0.7$; 7% vs. 5%, $P = 0.7$; and 5% vs. 5%, $P = 0.99$, respectively).

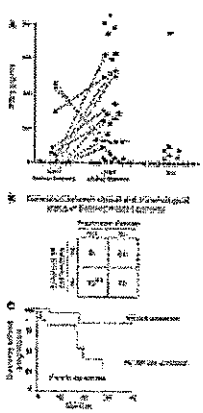

View larger version (17K): [in this window] [in a new window]

Figure 6

Correlation between NK cell activation and disease control in GIST patients. (A) Therapy with Gleevec-induced enhanced NK cell IFN-γ production. Blood NK cells were purified from GIST patients (Supplemental Table 1) at diagnosis after 2-12 months of therapy with 400 mg of Gleevec or from sex- and age-matched normal volunteers (NV) and cocultured with MD-DCs in the presence of LPS as described in Methods. Filled symbols correspond to individual patients or controls. Circles, objective responses; triangles; progressive disease. A longitudinal study enrolling 11 cases before and after Gleevec treatment is depicted with lines. Asterisk indicates significant differences between mean values of IFN-γ production after Gleevec compared with prior Gleevec or controls ($P < 0.05$) in 37 consecutive patients. (B) Correlation between clinical outcome and NK cell activation induced by therapy with Gleevec. The clinical responders exhibited stable disease, or partial or complete regressions (WHO criteria). The biological responders exhibited NK cell IFN-γ secretion above 130 pg/ml after at least 2 months of Gleevec therapy (cut-off defined according to the data shown in A). A significant correlation

between NK cell activation and clinical outcome at the time of NK cell activation assessment was found (**P = 0.03, Fisher's exact method). (C) NK cell activation is associated with prolonged time to progression in GIST patients treated with Gleevec. The study of the time to progression was performed for 43 patients with a median follow-up of 13.2 months. Patients who exhibited enhanced NK cell functions at 2 months of Gleevec (n = 22; red) and those who did not (n = 21; blue) (log rank test, P = 0.03).

To address the clinical relevance of the NK cell activation found after Gleevec administration in GIST patients, we assessed the sensitivity of gastrointestinal stromal tumor cells to NK cell lysis in vitro using a candidate GIST line. This GIST cell line was lysed by IL-2-activated NK cells purified from 7 different GIST-bearing patients at diagnosis. Similar lysis was obtained against the K562 NK cell sensitive target (Figure 7A). We also assessed the cytotoxic functions of freshly purified NK cells from 6 GIST patients, prior to and 2 months after Gleevec therapy (Figure 7B). Gleevec therapy significantly increased NK cell cytotoxicity. The NK cell recognition of GIST and K562 did not differ significantly. We found some molecular features shared by GISTs that could account for their potential NK cell sensitivity in vivo. More than half of the GISTs (9 out of 15; 60%) showed a complete deficiency in the transcription of TAP-1 mRNA, whereas most overexpressed the NKG2D ligands MHC class I-like MICB (4 out of 6), ULBP1 (5 out of 6), and ULBP3 (5 out of 6), compared with nontumoral gut tissue (Supplemental Table 2). These results were confirmed at the protein level by immunohistochemistry on 5 frozen GIST specimens using anti-MHC class I and anti-MICA/B mAb's and by Western blotting (data not shown). The relevance of the DC/NK cell cross-talk leading to NK cell activation in patients has been documented in the skin undergoing severe lichenoid dermatitis. Adverse cutaneous reactions induced by Gleevec are frequent, generally moderate, and dosage dependent (21). The skin was inflamed as evidenced by the presence of numerous mature DC-LAMP$^+$ DCs invading the dermis and of CD57$^+$ CD3$^-$ NK cells that eventually interacted (Figure 7B). These images are reminiscent of the DC/NK cell cross-talk first identified in the atopic dermatitis caused by skin malassezia (22).

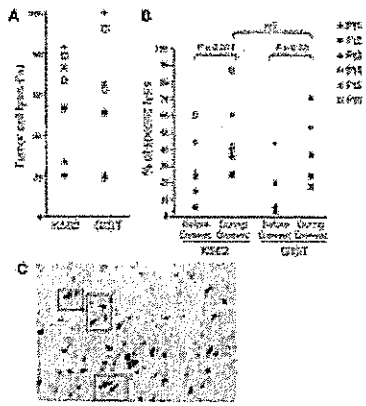

View larger version (51K):

[in this window]

[in a new window]

Figure 7

GISTs are NK cell-sensitive targets. (A) NK cell recognition of a GIST cell line. $CD3^-/CD56^+$ NK cells from GIST patients at diagnosis were activated overnight with 1000 IU rhuIL-2. The cytolytic activity of these NK cells was tested against the NK cell—sensitive K562 targets and against a GIST cell line in a ^{51}Cr release assay, using an E/T ratio of 10:1. Data represent the means of triplicate wells of 7 different GIST patients. Each symbol represents an individual patient's NK cell lysis of both targets (see key in B). (B) Gleevec promoted enhanced NK cell recognition of GIST cells. Experimental settings were the same as in A, but cytotoxicity assays had been performed before and 2 months after initiation of Gleevec therapy. (C) DC/NK cell cross-talk in a Gleevec-induced lichenoid dermatitis. Skin biopsies from a lichenoid dermatitis were taken from a patient bearing GISTs in complete regression after a year of oral administration of Gleevec. Formol-fixed and paraffin-embedded sections (4 μm thick) were immunohistochemically stained with an anti-DC-LAMP mAb (Schering-Plough Corp., Dardilly, France) and anti-CD57 mAb (NK1, Dako A/S, Glostrup, Denmark). Double-staining with anti-CD3 and anti-CD57 mAb demonstrated that $CD57^+$ cells were all $CD3^-$. $DC\text{-}LAMP^+$ mature dendritic cells were visualized by light microscope (brown staining). $CD57^+$ NK cells (3 black boxes) were identified by their red color and visible nuclei (x400 magnification).

Discussion

Gleevec is a paradigmatic pharmacological agent targeting specific mutations in protooncogenes (KIT/PDGFR/BCR/ABL) that is required for the malignant transformation of stromal cells of the gut (GIST) or myeloid precursors (chronic myeloid leukemia). The clinical breakthrough achieved with Gleevec in the management of irresectable GISTs or progressive chronic myelogenous leukemia (CML) has been approved worldwide (8, 9). However, this specific kinase inhibitor appears to promote antitumor effects even in tumors lacking target-activating mutations (Supplemental Table 1A). Here we highlight an alternate mode of action of Gleevec that is not tumor cell-autonomous and that involves host bone marrow-derived DCs. Indeed, we have identified the NK

cell-dependent antitumor effects promoted by Gleevec-treated DCs in mouse tumor models; our findings highlight the importance of Gleevec-mediated NK cell activation in patients bearing GISTs devoid of KIT/PDGFR mutations and displaying clinical responses to Gleevec.

Long-term exposure to Gleevec in mice endows host DCs with enhanced NK cell stimulatory capacity (Figure 4E), and such in vivo effects of Gleevec on host DCs can be dramatically augmented by coadministration of the DC growth factor FL in both NK cell activation (Figure 3, D and E) and NK cell-dependent antitumor activity (Figures 1 and 2). FL led to a marked increase in the frequency of $CD11c^+/KIT^+/CD11b^+$ DCs, the cell population that presumably responds to Gleevec (Supplemental Figure 3B). In addition, we found that FL could not be substituted for by G-CSF or GM-CSF in association with Gleevec for the expansion of $CD69^+/DX5^+/CD3^-$ NK cells in vivo (data not shown). The residual plasmatic concentrations of Gleevec following oral administration of Gleevec at 150 mg/kg bi-injection daily (bid) were 576 ng/ml (1 μM), corresponding to the IC_{50} concentration achieved in clinical trials with Gleevec (8). Plasma concentrations of Gleevec peaked at 6,020 ng/ml (60 μM) in FL+Gleevec, and they peaked at 12,177 ng/ml (120 μM) with Gleevec alone, which supports the hypothesis that DCs are pharmacological targets of Gleevec in vivo.

NK cells have recently been involved in the host-mediated control of cancer. The renaissance of interest in NK cells in tumor immunosurveillance can be attributed to the discovery of stress-induced ligands for receptors that activate NK cells (23-25) and to the relevance of interactions between MHC class I molecules and killer inhibitory receptors in mismatched hematopoietic transplants, which cause NK cell—mediated graft versus leukemia effects (26). Therefore, MHC class I or TAP loss tumor variants and tumors overexpressing NKG2D ligands are ideal targets for NK cell activity (23-29). Here we report that NK cell functions were enhanced in 49% of Gleevec-treated GIST patients. Our data suggest that Gleevec-mediated NK cell activation might play a part in tumor control either by synergizing with the cell-autonomous effect of Gleevec or by keeping tumors in check after the direct action of Gleevec on tumor cells. First, none of the 10 patients who had a progressive disease exhibited enhanced NK cell functions. Importantly, the time to progression was significantly longer in GIST patients for whom Gleevec caused NK cell activation than in patients without NK cell activation. Second, the GIST model bears molecular features of NK cell sensitivity, namely TAP-1 deficiency, loss of MHC class I molecules, high expression of NKG2D ligands (Supplemental Table 2> and data not shown), and GIST recognition by NK cells comparable to that of K562 (Figure 7A). Notably, in 50% of GIST-bearing patients, a fraction of circulating NK cells showed a downregulation of NKG2D expression at diagnosis (data not shown), which suggests that GISTs secrete soluble NKG2D ligands that might downregulate NKG2D expression on blood NK cells, similarly to the downregulation seen on T cells (30). Nonetheless, the relevance of NKG2D receptors in NK cell recognition of GISTs remains to be established. Moreover, we could not find any modulation of natural killer cytotoxicity receptor (NKp30, 44, 46) expression following Gleevec therapy in circulating NK cells (data not shown). We did not detect circulating IFN-γ, TNF-α, GM-CSF, IL-10, or IL-13 — all cytokines produced mostly by $CD56^{bright}$ CD16 NK cells — in any patients, whether or not they showed NK cell activation (data not shown).

The relevance of the DC/NK cell cross-talk is postulated in various physiopathological settings (22, 31–33) and has been demonstrated for the control of mouse tumors (10) and the murine cytomegalovirus viral replication in vivo (34). DCs and NK cells might interact in inflammatory lesions where chemokines and cytokines recruit both DCs and NK cells (35) or in the lymph nodes, where cooperation between IL-2-producing $CD4^+$ T cells and NK cells is ongoing (33). Knowledge of whether the Gleevec-conditioned DC/NK cell cross-talk is mediated in situ or at distant sites (lymphoid organs) remains elusive. Nevertheless, in one patient who benefited from therapy with Gleevec for one year, we found a DC/NK cell interaction in an unusual site (skin undergoing Gleevec-induced lichenoid dermatitis). This side effect regressed after removal of Gleevec, suggesting that the maturation of dermal DCs and/or recruitment of NK cells in the dermis was induced by Gleevec.

Any molecular mechanism accounting for NK cell triggering by Gleevec-stimulated DCs that does not imply the maturation of DCs (see Supplemental Figure 2) or the presence of IL-12 deserves comprehensive analysis. It is worth considering whether adoptive transfer of Gleevec-stimulated DCs or a combination of FL or NK cell-stimulating factors to Gleevec could be suitable therapeutic options in the clinicians' armamentarium against hitherto untreatable NK cell-dependent malignancies or infectious diseases.

▲Top
▲Abstract
▲Introduction
▲Results
▲Discussion
▪ Methods
▼References

Methods

Patients

Patients enrolled in the French phase II trial (Institut Gustave Roussy (IGR)/Centre Léon Bérard, Novartis Pharmaceuticals Corp., East Hanover, New Jersey, USA) testing the efficacy of STI571 (imatinib mesylate, Gleevec; formerly called CGP57148; Novartis Pharmaceuticals Corp.). Gleevec in GISTs were studied according to the protocols approved for the follow-up of the patients' immunomonitoring by the local research and ethical committee (Comité Consultatif pour la Protection des Personnes Participant à une Recherche Biomédicale).

Peripheral blood (60 ml) was drawn from GIST patients before and 2–6 months after treatment with Gleevec (400 mg/day) for purification of NK cells. Age– and sex–matched normal volunteers were chosen for control studies. Patients' characteristics are described in Supplemental Table 1B. Tumor response was assessed by computed tomography (CT) scan with response classified according to WHO criteria at 2 and 12 months after the beginning of treatment. Nonprogressive disease comprised stable disease and objective partial or complete responses.

Mice

Female C57BL/6 (H–2^b) wild–type or $Rag2^{-/-}$ mice and female BALB/c SCID (H–2^d) mice were obtained from the Center d' Elevage Janvier (Le Genest St. Isle, France) and the Center d' Elevage Iffa Credo (L' Arbresle, France) and maintained in the Animal Facility of Institute Gustave Roussy according to the animal experimental ethics committee guidelines of the facility. $Swiss^{nu/nu}$ mice were maintained at the IGR animal facility. Mast cell–deficient ($WBB6F1^{W/Wv}$) (W/Wv) and control congenic mast cell–sufficient ($WBB6F1^{+/+}$) (WT) mice were raised at the Institut Pasteur animal facility (Paris, France). The original stocks of parental strains (i.e., WB–W/+ and C57BL/6–W^v/+) were obtained from The Jackson Laboratory (Bar Harbor, Maine, USA). BM mast cells derived from W/Wv mice, which lack tissue mast cells due to a point mutation at position 660 of the c–kit sequence (17, 18), exhibit markedly reduced phosphorylation of the KIT molecule upon stimulation with stem cell factor (SCF). All female mice were used at 6–––25 weeks of age.

Generation of dendritic cells in vitro

Mouse BM–DCs. BM–DCs were propagated from BM progenitor cells of WT or W/Wv mice in culture medium supplemented with 1,000 IU/ml of rmGM–CSF (R & D Systems, Minneapolis, Minnesota, USA) and 1,000 IU/ml of rmIL–4 (R & D Systems) as previously described (12). Culture medium was renewed at days 2 and 4. DCs were harvested on day 5 or 6, spun down, and transferred into new 6–well plates (referred to as "day 7 DC" henceforth). To modulate BM–DC phenotype, cultures of BM–DCs were incubated in Gleevec (10^{-6} M, 10^{-8} M or 10^{-10} M; neosynthetized by C. Auclair, Institut Gustave Roussy) on day 5 or 6 of culture for 20 hours before use. For phenotypic analyses, cells were incubated with FITC–conjugated anti–I–A^b (AF6–120.1) and PE–conjugated anti–CD11c (HL–3); FITC–conjugated CD86 (GL1), CD40 (3/23), H–2Kb (AF6–885); and PE–conjugated anti–CD80 (16–10A1), H–2Db (KH95). All antibodies were purchased from BD Biosciences — Pharmingen (San Diego, California, USA). Cells were gated according to size and granulosity with exclusion of propidium iodide–positive cells. Residual B lymphocytes ($B220^+$ cells) and granulocytes ($Gr1^+$ cells) were detected in the $CD11c^-$/$I–A^{b-}$ cells and constituted less than 20% of the total cell population. T cells and NK cells were not propagated in these DC culture conditions. BM–DCs derived from loss–of–function mice (W/Wv) were analyzed for MHC class I expression and exhibited levels of MHC class II, CD80, CD86, and CD40 expression comparable to those of wild–type BM–DCs.

Human $CD34^+$–derived DCs. G–CSF–mobilized human peripheral blood stem cells from normal volunteers or patients were isolated and subjected to sorting of $CD34^+$ progenitors (MACS system, CD34 selection kit; Miltenyi Biotec GmbH, Bergisch–Gladbach, Germany). Half a million cells were propagated in 96–well plates using RPMI1640

(Life Technologies, Cergy Pontoise, France) supplemented with 2 mM L-glutamine, 100 IU/ml penicillin, 100 µg/ml streptomycin (Life Technologies), 10% heat-inactivated, endotoxin-free fetal calf serum (PAN Biotech GmbH, Aidenbach, Germany) and a cocktail of cytokines, including SCF (25 ng/ml; Amgen, Thousand Oaks, California, USA), rhuGM-CSF (1,000 IU/ml, Leucomax, Schering-Plough, Levallois-Perret, France), and rhuTNF-α (25 ng/ml, Boehringer Ingelheim GmbH, Mannheim, Germany), herein referred to as complete medium, for 13 days. Complete medium was renewed every 3 or 4 days and cells were expanded at a concentration of 0.5 x 10^6/ml. Gleevec was added to culture medium at day 12 for 20 hours before use in NK cell bioassays.

Preparation of NK cells

Mouse NK cells. Splenocytes were harvested from BL6-Rag2$^{-/-}$ or BALB/c SCID mice. Splenic nonadherent cells were generated by subjecting red blood cell-deprived splenocytes to 3 hours of adherence at 37° C. Nonadherent cells were analyzed by FACS using monoclonal antibodies to CD3-FITC, NK1.1-PE, DX5-PE, or CD69CyC prior to coculture with BM-DCs. Up to 40% of such splenocytes were CD3$^-$/DX5$^+$.

Human NK cells. Purified (85-95% CD56$^+$/CD3$^-$) resting NK cells were obtained from peripheral blood lymphocytes from normal volunteers or GIST patients by magnetic cell separation (Miltenyi Biotech) using a two-step protocol: PBMCs were first incubated with hapten-conjugated monoclonal antibodies to CD3, CD14, CD19, CD36, and IgE for 30 minutes followed by negative selection with MACS antihapten microbeads (Miltenyi Biotech).

Preparation of DC/NK cell cocultures

Procedures have been previously described (12, 19). Main principles are described in the figure legends.

Mouse cocultures. Culture medium used was RPMI1640-based complete medium containing 10% heat-inactivated bovine serum for mouse cultures and RPMI1640 + 10% heat-inactivated pooled ABS for human cocultures. NK cells (human CD3$^-$/CD56$^+$ or mouse splenocytes from immunodeficient mice) were seeded at 10^5/well in 96-well plates for 40 hours (human cocultures) or 20 hours (mouse cocultures). DC/NK ratios of mouse cocultures were 0.5:1.0 (unless otherwise specified) and 1:25 for human cocultures or as specified in figure legends. Mouse BM-DC/NK cocultures were performed in an allogeneic (B6/BALB/c or WBB6F1$^{W/Wv}$/BALB/c or Rag2$^{-/-}$BL6, WBB6F1^{WT}/BALB/c or Rag2$^{-/-}$BL6) or syngeneic (B6/B6) system.

Human cocultures. Human immature MD-DCs were propagated from normal volunteers' peripheral monocytes in rhGM-CSF (1,000 IU/ml) + rhIL-4 (1,000 IU/ml) in AIMV at 3 x 10^5 cells/ml without serum and frozen at day 5, and subsequently thawed for 2 days in complete medium before coculture with allogeneic NK cells (normal volunteers or GIST patients). FACS analysis showing expression of CD1a, CD11c, and DC-SIGN, low levels of HLA-DR, CD80, and CD40, and lack of expression of CD83 confirmed their immature phenotype. Quality control parameters of MD-DCs included mixed lymphocyte reactions in the presence or absence of LPS. NK cells were cocultured with allogeneic immature DCs for 40 hours in 10% pooled AB serum at a ratio of 1:1 in the presence of 1 µg/ml LPS (19).

Assessment of NK cell effector functions

Cytotoxicity assays. Cells from 20-hour cocultures were collected. Viable NK cells that were stained with trypan blue (Life Technologies) were counted and used as effector cells. Cytotoxicity of NK cells was measured in a standard 4-hour ^{51}Cr-release assay using $Na_2{}^{51}CrO_4$-labeled K562 (human cocultures) or YAC-1 targets (mouse cocultures). Experiments were conducted in triplicate at various effector/target (E/T) ratios. In some experiments, target cells were a GIST cell line provided by J.A. Fletcher.

Cytokine detection and quantification (IFN-γ). After DC/NK coculture, supernatants were harvested, stored at -80° C, and then assessed either directly or after 2-10 times dilution using commercial ELISA kits (as noted in figure legends) (BD Biosciences — Pharmingen).

Assessment of in vivo NK cell functions

C57BL/6 mice or Swiss$^{nu/nu}$ phenotype were subjected to intraperitoneal administration of FL (10 μg/mouse/day for 10 days) (kindly provided by Immunex Corp., Seattle, Washington, USA) along with oral feeding of PBS or Gleevec (150 mg/kg bid) for the last 4 days. Negative control mice received PBS intraperitoneally and orally only, and positive control mice were injected intraperitoneally with rhIL-2 (Roussel Uclaf, Romainville, France) at 10^5 IU/mouse, bid for 4 days. Mice were sacrificed at day 11 to examine CD69 expression levels on $DX5^+/CD3^-$ (non-BL6 background) or $NK1.1^+/CD3^-$ NK cells on splenocytes. Cells were enumerated using trypan blue exclusion prior to immunostaining with three-color mAb's (anti-CD3 FITC, anti-DX5-PE or anti-NK1.1-PE, and anti-CD69CyC).

Tumor models

RMA is a Rauscher's virus-induced lymphoma cell line derived from B6, and RMA-S is a TAP-defective variant of RMA. One million cells of each tumor line were injected subcutaneously into each flank of C57BL/6 mice, and tumor growth was monitored biweekly in each treatment group. AK7 is an asbestos-induced mesothelioma from C57BL/6 mice, as previously described (12) MCA102 is a methylcholanthrene-induced sarcoma and B16F10 is a melanoma; both are from a C57BL/6 background (kindly provided by M.T. Lotze, University of Pittsburgh, Pittsburgh, Pennsylvania, USA). YAC-1 is a Moloney leukemia virus-induced lymphoma cell line from A/Sn (H-2a) mice.

Statistical analyses

Results are expressed as means ± SEM or as ranges when appropriate. Groups were compared by using analysis of variance (ANOVA) followed by multiple comparison of means with Fischer's least-significance procedure. When the variables studied were not normally distributed, nonparametric statistical methods were used. The Wilcoxon two-sample rank sum test was used to compare the values of continuous variables between two groups. When three or more groups were compared, the Kruskall-Wallis test was used. Paired comparisons were made using Wilcoxon's paired test. P values less than 0.05 were considered significant.

Acknowledgments

M. Terme has received a fellowship from the Ligue Française Contre le Cancer. C. Borg was supported by the Hospices Civils de Lyon and by the Association pour la Recherche Contre le Cancer (ARC). We are indebted to Novartis Pharmaceuticals Corp. for the authorization given to IGR to assess the NK cell effector functions of patients in the phase II trial. This work has also been supported by INSERM, the ARC and LIGUE Labellisée Française Contre le Cancer, and a European Community Contract 503319 Allostem grant. We are more than grateful to Alain Deroussent, the core facility for mass spectrometry, Institut Fédératif de Recherche 54, and to the patients who participated. We thank Micheline Hadjard for her incredible devotion in harvesting and collecting patient specimens. We remain indebted to the IGR Animal Facility Staff for technical help.

Footnotes

C. Borg, M. Terme, and J. Taïeb contributed equally to this work.

Nonstandard abbreviations used: bi-injection daily (bid); bone marrow–derived DC (BM-DC); break point cluster region/Abelson leukemia virus (BCR/ABL); chronic myelogenous leukemia (CML); c-kit loss-of-function mutation (W/Wv); fms-like tyrosine 3 kinase ligand (FL); gastrointestinal stromal tumor (GIST); progression-free survival (PFS); stem cell factor (SCF); transporter associated with antigen processing (TAP).

Conflict of interest: The authors have declared that no conflict of interest exists.

References

1. Rubin, B.P. et al. 2001. KIT activation is a ubiquitous feature of gastrointestinal stromal tumors. *Cancer Res.* 61:8118–8121.[Abstract/Free Full Text]

2. Heinrich, M.C. et al. 2003. PDGFRA activating mutations in gastrointestinal stromal tumors. *Science.* 31:708–710.[CrossRef]

3. Apperley, J.F. et al. 2002. Response to imatinib mesylate in patients with chronic myeloproliferative diseases with rearrangements of the platelet–derived growth factor receptor beta. *N. Engl. J. Med.* 347:481–487.[Abstract/Free Full Text]

4. Buchdunger, E., O' Reilly, T., and Wood, J. 2002. Pharmacology of imatinib (STI571). *Eur. J. Cancer.* 38:S28–S36.[Medline]

5. Heinrich, M.C., Blanke, C.D., Druker, B.J., and Corless, C.L. 2002. Inhibition of KIT tyrosine kinase activity: a novel molecular approach to the treatment of KIT–positive malignancies. *J. Clin. Oncol.* 20:1692–1703.[Abstract/Free Full Text]

6. Demetri, G.D. et al. 2002. Efficacy and safety of imatinib mesylate in advanced gastrointestinal stromal tumors. *N. Engl. J. Med.* 347:472–480.[Abstract/Free Full Text]

7. Heinrich, M.C. et al. 2003. Kinase mutations and imatinib response in patients with metastatic gastrointestinal stromal tumor. *J. Clin. Oncol.* 21:4342–4349.[Abstract/Free Full Text]

8. Cohen, M.H. et al. 2002. Approval summary for imatinib mesylate capsules in the treatment of chronic myelogenous leukemia. *Clin. Cancer. Res.* 8:935–942.[Abstract/Free Full Text]

9. Bauer, S. et al. 2003. Response to imatinib mesylate of a gastrointestinal stromal tumor with very low expression of KIT. *Cancer Chemother. Pharmacol.* 51:261–265.[Medline]

10. Fernandez, N.C. et al. 1999. Dendritic cells (DC) promote natural killer (NK) cell functions: dynamics of the human DC/NK cell cross talk. *Nat. Med.* 5:405–411.[CrossRef][Medline]

11. Glas, R. et al. 2000. Recruitment and activation of natural killer (NK) cells in vivo determined by the target cell phenotype. An adaptive component of NK cell–mediated responses. *J. Exp. Med.* 191:129–138.[Abstract/Free Full Text]

12. Seaman, W.E., Sleisenger, M., Eriksson, E., and Koo, G.C. 1987. Depletion of natural killer cells in mice by monoclonal antibody to NK–1.1. Reduction in host defense against malignancy without loss of cellular or humoral immunity. *J. Immunol.* 138:4539–4544.[Abstract/Free Full Text]

13. Colucci, F., and Di Santo, J.P. 2000. The receptor tyrosine kinase c-kit provides a critical signal for survival, expansion, and maturation of mouse natural killer cells. *Blood.* 95:984-991.[Abstract/Free Full Text]

14. Maraskovsky, E. et al. 1996. Dramatic increase in the numbers of functionally mature dendritic cells in Flt3 ligand-treated mice: multiple dendritic cell subpopulations identified. *J. Exp. Med.* 184:1953-1962.[Abstract]

15. Gerosa, F. et al. 2002. Reciprocal activating interaction between natural killer cells and dendritic cells. *J. Exp. Med.* 195:327-333.[Abstract/Free Full Text]

16. Sun, X., Layton, J.E., Elefanty, A., and Lieschke, G.J. 2001. Comparison of effects of the tyrosine kinase inhibitors AG957, AG490, and STI571 on BCR-ABL-expressing cells, demonstrating synergy between AG490 and STI571. *Blood.* 97:2008-2015.[Abstract/Free Full Text]

17. Nocka, K. et al. 1990. Molecular bases of dominant negative and loss of function mutations at the murine c-kit/white spotting locus: W37, Wv, W41 and W. *EMBO J.* 9:1805-1813.[Abstract]

18. Kitamura, Y., Matsuda, H., and Hatanaka, K. 1979. Clonal nature of mast-cell clusters formed in W/Wv mice after bone marrow transplantation. *Nature.* 281:154-155.[Medline]

19. Fernandez, N.C. et al. 2002. Dendritic cells (DC) promote natural killer (NK) cell functions: dynamics of the human DC/NK cell cross talk. *Eur. Cytokine Netw.* 13:17-27.[Medline]

20. Van Glabbeke, M.M. et al. 2003. Prognostic factors of toxicity and efficacy in patients with gastro-intestinal stromal tumors (GIST) treated with imatinib: A study of the EORTC-STBSG, ISG and AGITG [abstract]. *Proc. Am. Soc. Clin. Oncol.* 22:3286.

21. Valeyrie, L. et al. 2003. Adverse cutaneous reactions to imatinib (STI571) in Philadelphia chromosome-positive leukemias: a prospective study of 54 patients. *J. Am. Acad. Dermatol.* 48:201-206.[CrossRef][Medline]

22. Buentke, E. et al. 2002. Natural killer and dendritic cell contact in lesional atopic dermatitis skin-Malassezia-influenced cell interaction. *J. Invest. Dermatol.* 119:850-857.[Abstract/Free Full Text]

23. Diefenbach, A., Jensen, E.R., Jamieson, A.M., and Raulet, D.H. 2001. Rae1 and H60 ligands of the NKG2D receptor stimulate tumour immunity. *Nature.* 413:165-171.[CrossRef][Medline]

24. Cerwenka, A., Baron, J.L., and Lanier, L.L. 2001. Ectopic expression of retinoic acid early inducible-1 gene (RAE-1) permits natural killer cell-mediated rejection of a MHC class I-bearing tumor in vivo. *Proc. Natl. Acad. Sci. U. S. A.* 20:11521-11526.[CrossRef]

25. Lanier, L.L. 2001. A renaissance for the tumor immunosurveillance hypothesis. *Nat. Med.* 11:1178-1180.[CrossRef]

26. Ruggeri, L. et al. 2002. Effectiveness of donor natural killer cell alloreactivity in mismatched hematopoietic transplants. *Science.* 295:2097-2100.[Abstract/Free Full Text]

27. Salcedo, M., Momburg, F., Hammerling, G.J., and Ljunggren, H.G. 1994. Resistance to natural killer cell lysis conferred by TAP1/2 genes in human antigen-processing mutant cells. *J. Immunol.* 152:1702-1708.[Abstract/Free Full Text]

28. Bauer, S. et al. 1999. Activation of NK cells and T cells by NKG2D, a receptor for stress-inducible MICA. *Science.* 285:727-729.[Abstract/Free Full Text]

29. Cosman, D. et al. 2001. ULBPs, novel MHC class I-related molecules, bind to CMV glycoprotein UL16 and stimulate NK cytotoxicity through the NKG2D receptor. *Immunity.* 14:123-133.[Medline]

30. Groh, V., Wu, J., Yee, C., and Spies, T. 2002. Tumour-derived soluble MIC ligands impair expression of NKG2D and T-cell activation. *Nature.* 419:734-738.[CrossRef][Medline]

31. Moretta, A. 2002. Natural killer cells and dendritic cells: rendezvous in abused tissues. *Nat. Rev. Immunol.* 2:957-964.[CrossRef][Medline]

32. Zitvogel, L. 2002. Dendritic and natural killer cells cooperate in the control/switch of innate immunity. *J. Exp. Med.* 195:F9-F14.[CrossRef][Medline]

33. Fehniger, T.A. et al. 2003. $CD56^{bright}$ natural killer cells are present in human lymph nodes and are activated by T cell-derived IL-2: a potential new link between adaptive and innate immunity. *Blood.* 101:3052-3057.[Abstract/Free Full Text]

34. Andrews, D.M., Scalzo, A.A., Yokoyama, W.M., Smyth, M.J., and Degli-Esposti, M.A. 2003. Functional interactions between dendritic cells and NK cells during viral infection. *Nat. Immunol.* 4:175-181.[CrossRef][Medline]

35. Mantovani, A., Gray, P.A., Van Damme, J., and Sozzani, S. 2000. Macrophage-derived chemokine (MDC). *J. Leukoc. Biol.* 68:400-404.[Abstract/Free Full Text]

Available online at www.sciencedirect.com
SCIENCE DIRECT®
Immunology Letters 92 (2004) 227–235
Immunology Letters
www.elsevier.com/locate/

The mouse natural killer T cell-associated antigen recognized by U5A2-13 monoclonal antibody is intercellular adhesion molecule-1

Atsushi Shimizu [a,e], Hiroki Sasaki [b], Kazuhiko Aoyagi [b], Mitsuzi Yoshida [a], Kazunori Kato [a], Yuji Heike [a,c], Yoshinori Ikarashi [a], Kazuo Shirakawa [a], Yoichi Takaue [c], Atsushi Miyajima [d], Masaaki Terada [b], Hideo Nagai [e], Hiro Wakasugi [a,*]

[a] *Pharmacology Division, National Cancer Center Research Institute, Tsukiji 5-1-1, Chuo-ku, Tokyo 104-0045, Japan*
[b] *Genetics Division, National Cancer Center Research Institute, Tokyo 104-0045, Japan*
[c] *Department of Medical Oncology, Hematopoietic Stem Cell Transplant/Immuno Therapy Division, National Cancer Center Hospital, Tokyo 104-0045, Japan*
[d] *Laboratory of Cell Growth and Differentiation, Institute of Molecular and Cellular Sciences, University of Tokyo, Tokyo 113-0032, Japan*
[e] *Department of Surgery, Jichi Medical School, Tochigi 329-0498, Japan*

Received 19 November 2003; received in revised form 5 January 2004; accepted 11 January 2004

Abstract

Natural Killer T (NKT) cells in mice are generally defined as NK1.1$^+$ T cells, although NK1.1 antigen is expressed only in C57BL/6 and related strains. This has precluded investigations of other strains. To find a novel NKT cell surface marker, we generated a monoclonal antibody (mAb), U5A2-13, which recognizes phenotypically and functionally similar populations to NKT cells in naïve mice irrespective of strain. Here, by using a COS-7 expressional cloning system, we molecularly cloned a cDNA encoding a protein reactive with the U5A2-13 mAb and then identified it as intercellular adhesion molecule-1 (ICAM-1). Importantly, the U5A2-13 mAb did not stain hepatic mononuclear cells from ICAM-1 gene disrupted mice. Furthermore, Pepscan method disclosed that the discontinuous epitope for U5A2-13 mAb is composed of three loops located in extracellular domain two of ICAM-1. Overall, U5A2-13, a mAb originally established for mouse NKT cells, recognizes a novel conformational epitope of ICAM-1.

Keywords: Natural killer T cell; U5A2-13 monoclonal antibody; Intercellular adhesion molecule-1; Molecular cloning

1. Introduction

Natural Killer T (NKT) cells in mice are usually defined as lymphocytes expressing intermediate levels of TCR and NK cell-associated molecules, particularly NK1.1. They predominantly express TCR with invariant Vα14Jα281 and Vβ8, 7, or 2, and most of them are phenotypically double negative (CD4$^-$CD8$^-$) or single positive (CD4$^+$CD8$^-$) T cells [1–6]. These cells produce large amounts of IFN-γ and IL-4, suggesting that they play an important role in regulating the Th1/Th2 balance [1,2,7–11]. NKT cells are potentiated by α-galactosylceramide (α-GalCer) to produce these cytokines in a CD1d dependent manner [7,8,10,12–17]. NK1.1 antigen is expressed on NK and NKT cells in only C57BL/6 and a few related strains. Therefore, studies of NKT cells in NK1.1-negative strains are quite limited by the lack of markers that can reliably enumerate the population [1,2]. Earlier studies have also shown that NK1.1$^+$CD4$^+$ T cells lose NK1.1 expression upon in vitro activation [18].

Several surrogate markers such as CD44, Ly6C, Ly49A and DX5 have been postulated. However, these molecules do not accurately encompass NKT cells in C57BL/6 mice and their specificity is difficult to determine [2]. An antibody (Ab) to Vα14$^+$ TCR [19] stained less than 20% of Vα14$^+$Jα281$^+$NK1.1$^+$ T cells in thymocytes and is no more used [6]. While tetrameric CD1d molecules loaded with α-GalCer have been used recently to specifically detect Vα14 NKT cells [20,21], NKT cells detected with these tetramers might receive positive signals and become

* Corresponding author. Tel.: +81-3-3547-5248; fax: +81-3-3542-1886.
E-mail address: hwakasug@gan2.ncc.go.jp (H. Wakasugi).

0165-2478/$ – see front matter © 2004 Elsevier B.V. All rights reserved.
doi:10.1016/j.imlet.2004.01.005

activated, making it difficult to ascertain the physiological role of NKT cells in vivo. Furthermore, NKT cells are heterogeneous and, regardless of NK1.1 expression, consist of CD1d dependent and independent subsets [22–27].

To overcome these limitations, we established the monoclonal antibody (mAb), U5A2-13, which selectively identifies populations similar to NK1.1$^+$ T cells in both NK1.1-positive and -negative mouse strains [28]. U5A2-13 mAb was originally obtained by immunizing a Fischer rat with tMK-2U lymphoma cells from a BALB/c nude mouse carrying a xenografted human inflammatory breast tumor [29]. We have shown that U5A2-13$^+$ T cells use an invariant TCR Vβ8, 7, or 2 predominantly and that, similar to NK1.1$^+$ T cells, U5A2-13$^+$ T cells can produce both IFN-γ and IL-4 upon cross-linking with CD3 [30]. We also demonstrated that hepatic U5A2-13$^+$ T cells recognize the NKT cell ligand, α-GalCer, presented by CD1d molecules on dendritic cells [31]. These results indicated that U5A2-13 mAb would be a valuable tool in the study of NKT cells in NK1.1-negative mouse strains.

However, the cell surface molecule recognized by U5A2-13 mAb was unknown. To elucidate the novel cell surface marker constitutively expressed on NKT cells, we molecularly cloned the antigen and identified a new epitope of ICAM-1 on NKT cells, The conformational epitope is composed of three loops located in extra-cellular domain two of ICAM-1.

2. Materials and methods

2.1. Mice

Specific pathogen-free female C57BL/6 wild-type mice (Charles River Japan, Inc., Kanagawa, Japan) and ICAM-1 mutant mice (tm1Bay and tm1Jcgr; Jackson Laboratory, Bar Harbor, ME) maintained in the animal facility of the National Cancer Center Research Institute were studied at 8–12 weeks of age. All animal experiments were conducted in accordance with protocols approved by the institutional review board.

2.2. Antibodies and reagents

FITC-conjugated mAbs specific for mouse CD3 (145-2C11) and ICAM-1 (3E2), PE-conjugated control rat IgG2a (R-35-95), PE-conjugated U5A2-13, PE-conjugated anti-ICAM-1 (3E2), PerCP-conjugated streptavidin, biotinylated anti-CD3 (145-2C11) and anti-mouse Fcγ II/III receptor (2.4G2) were purchased from BD PharMingen (San Diego, CA) for flow cytometry. PE-conjugated anti-NK1.1mAb, and PE-conjugated anti-rat IgG2a were obtained from Caltag (Burlingame, CA).

Anti-ICAM-1 Ab (goat polyclonal IgG, M-19) was purchased from Santa Cruz Biotechnology (Santa Cruz, CA), and peroxidase-conjugated anti-goat IgG was obtained from Sigma Aldrich (Saint Louis, MO) for Western blotting and immunoprecipitation.

2.3. Cell cultures

The mouse B cell leukemia cell line, BCL1, was cultured in RPMI 1640 (Nissui Pharmaceutical Co. Ltd., Tokyo, Japan) medium supplemented with 10% heat inactivated FCS (JRH Biosciences, Lenexa, KS), 1 mM sodium pyruvate, 100 IU/ml penicillin, 100 μg/ml streptomycin, 50 μM 2-ME. COS-7 cells were maintained in DMEM supplemented with 10% heat inactivated FCS.

2.4. Construction of cDNA library

We isolated the gene encoding the antigen recognized by U5A2-13 mAb, using an expressional cloning strategy with COS-7 cells (African green monkey kidney cells expressing the T antigen of simian virus 40) [32]. The cloning source was the murine cell line BCL1, which was cultured in RPMI 1640 with 10% heat inactivated FCS. The cells were harvested for total RNA isolation using guanidinium thiocyanate. Poly(A)$^+$ RNA was selected by oligo(dT)-cellulose column chromatography and converted to double-stranded cDNA using oligo(dT) primers containing a *Not* I site. An *Eco*R I adapter was attached and cDNAs greater than 2.0 kb were fractionated by agarose gel electrophoresis, digested with *Not* I and ligated into the *Eco*R I/*Not* I-cleaved pME18S vector (simian virus 40-based mammalian expression vector; GenBank accession no. AB009864) [33]. Transfection into competent DH10B *E. coli* cells yielded approximately 1.0×10^6 independent cDNA clones.

2.5. Screening the cDNA library

DH10B cells carrying the plasmids were fused to COS-7 cells as described by Seed and Aruffo [32]. Three days after fusion, COS-7 cells were detached from the plate by incubation with PBS containing 5 mM EDTA. Cells were collected by centrifugation and resuspended in staining buffer (SB) (PBS containing 5% FCS, 0.5 mM EDTA and 0.05% NaN_3). PE-conjugated U5A2-13 mAb was added and the suspension was incubated at 4 °C for 30 min. The cells were washed three times and resuspended in SB. One percent of the most brightly stained cells were sorted using the fluorescence-activated cell sorter (FACS®) Vantage [34]. Plasmid DNA was recovered from the sorted cells and used to transform DH10B *E. coli* cells by electroporation. The transformants were cultured and spheroplast-fused with COS-7 cells for the next round of enrichment. Fourteen colonies were randomly selected after two rounds of enrichment and plasmid DNA was extracted from each colony. Plasmid DNAs purified from these 14 cDNA clones were individually transfected into COS-7 cells using Lipofectamin Plus® (Gibco Invitrogen, Carlsbad, CA) and analyzed by flow cytometry. Only one transfectant among the cDNA

clones, BLV-13, bound U5A2-13 mAb but not control rat IgG2a.

2.6. DNA sequencing

Both strands of the BLV-13 cDNA clone with an insert of 2.8 kb were sequenced with synthetic oligonucleotide primers and analyzed with an automated fluorescent DNA sequencer (Applied Biosystems, Foster City, CA). Nucleotides and deduced amino acids were analyzed by comparison with the GenBank database.

2.7. Southern blotting

Plasmid DNA (100 ng) purified from each screened cDNA library was digested with *Eco*R I/*Not* I, resolved by electrophoresis and blotted onto nitrocellulose membranes by alkaline transfer. A hybridization probe of 2.8 kb prepared by PCR using 100 pg BLV-13 cDNA as a template was labeled and detected using the commercially available DIG.High Prime DNA Labeling and Detection Starter Kit® (Roche; Mannheim, Germany), according to the manufacturer's instructions.

2.8. Western blotting, cell surface biotinylation and immunoprecipitation

The expression of ICAM-1 in COS-7 cells was assessed via immunoblot assay as described [35]. Cell surface proteins of the transfected COS-7 cells were biotinylated using sulfosuccinimidobiotin [36]. After three washes in PBS, cells were suspended at a density of 25×10^6/ml in 0.9% NaCl with 0.01 M HEPES (pH 8.0) and 0.5 mg/ml of Sulfo-NHS-biotin® (Pierce, Rockford, IL) and rocked for 30 min at room temperature. The reaction was terminated by adding 1 M Tris–HCl (pH 7.5) and incubated for an additional 15 min. After centrifugation, cells were disrupted in lysis buffer containing 50 mM Tris–HCl (pH 8.0), 150 mM NaCl and 1% Triton X-100 in the presence of the protease inhibitors aprotinin (2 μg/ml), leupeptin (2 μg/ml) and phenylmethylsulfonyl fluoride (PMSF) (0.57 mM) at 4 °C for 30 min with occasional mixing. After centrifugation, the supernatant served as the cell lysate. The cell lysate was clarified by an incubation with protein G-Sepharose® (Pharmacia, Peapack, NJ), immunoprecipitated with U5A2-13 mAb and anti-ICAM-1 polyclonal Ab for 2 h, then incubated again with protein G-Sepharose for 1 h. After five washes with lysis buffer, protein was eluted directly by boiling for 5 min in SDS sample buffer. The immunoprecipitates were resolved by 7.5% of SDS-PAGE and electrophoretically transferred onto Immobilon® membranes (Millipore, Bedford, MA). Biotinylated protein was detected using avidin and biotinylated horseradish peroxidase macromolecular complex (Vector, Burlingame, CA) and an Enhanced Chemiluminescence (ECL®) kit (Amersham, Aylesbury, UK).

2.9. Cell preparations and flow cytometry

Hepatic mononuclear cells (MNCs) were prepared as described [30]. The liver was removed, pressed through 200 μm gauge stainless steel mesh and suspended in RPMI 1640 containing 5% heat inactivated FCS. After washing with the same medium, the cells were resuspended in 30% Percoll® (Amersham Pharmacia Biotech, Uppsala, Sweden) and 65 U/ml heparin and centrifuged at $750 \times g$ for 15 min at room temperature. The cell pellet was collected and erythrocytes in the hepatic MNC suspension were removed using 0.83% ammonium chloride–Tris buffer. The remaining hepatic MNCs were washed in RPMI 1640 and suspended in SB. Except for when anti-rat IgG-PE was used, the cells were incubated beforehand with Fc-block reagent (2.4G2, anti-CD16/32, BD PharMingen). Hepatic MNCs (1×10^6) were incubated with FITC or PE conjugated mAbs for 30 min at 4 °C, then washed and suspended in SB for analysis using a FACS Calibur® and Cell Quest® software (Becton Dickinson, Mountain View, CA). Except for three-color examinations, cells were gated with propidium iodide (PI). Indirect staining proceeded as described [30].

2.10. Epitope mapping

Peptides were synthesized to include all overlapping linear 30-mers covering the whole mouse ICAM-1 sequence. We also designed peptides in which loops of the five domains were combined in all kinds of orientations, re-creating discontinuous regions of the Ig-like domains. The binding activities of U5A2-13 mAb to these peptides were measured by Pepscan Systems (Lelystad, The Netherlands). Briefly, 2230 overlapping 30-mers, off-set one by one, were synthesized and screened using credit-card format mini-PEPSCAN cards (455 peptide format/card) as described previously [37–39]. The binding of antibody to each peptide was tested in a PEPSCAN-based enzyme-linked immuno assay (ELISA). The 455-well credit-card format polyethylene cards, containing the covalently linked peptides, were incubated with antibody U5A2-13 (10 μg/ml, diluted in blocking solution which contains 5% horse-serum (v/v) and 5% ovalbumin (w/v) and 0.05% Tween 20) (4 °C, overnight). After washing the peptides were incubated with anti-rat IgG horseradish peroxidase (dilution 1/1000 in blocking solution) (1 h, 25 °C), and subsequently, after washing the peroxidase substrate 2,2′-azino-di-3-ethylbenzthiazoline sulfonate (ABTS) and 2 ul/ml 3% H_2O_2 were added. After 1 h the color development was measured. The color development of the ELISA was quantified with a CCD-camera and an image processing system. The setup consists of a CCD-camera and a 55 mm lens (Sony CCD Video Camera XC-77RR, Nikon micro-nikkor 55 mm f/2.8 lens), a camera adaptor (Sony Camera adaptor DC-77RR) and the Image Processing Software package Optimas, version 6.5 (Media Cybernetics,

Silver Spring, MD, USA). Optimas runs on a Pentium II computer system.

The identified reacting peptides were colored in a three-dimensional model of whole mouse ICAM-1, 1ic1.pdb, which was derived from the PDB-database [40] and was visualized using the software package Swiss PDB-viewer 3.7b1.

3. Results

3.1. Molecular cloning of a full-length cDNA encoding the antigen recognized by U5A2-13 mAb

We applied an expressional cloning strategy using COS-7 cells to isolate the gene encoding the antigen recognized

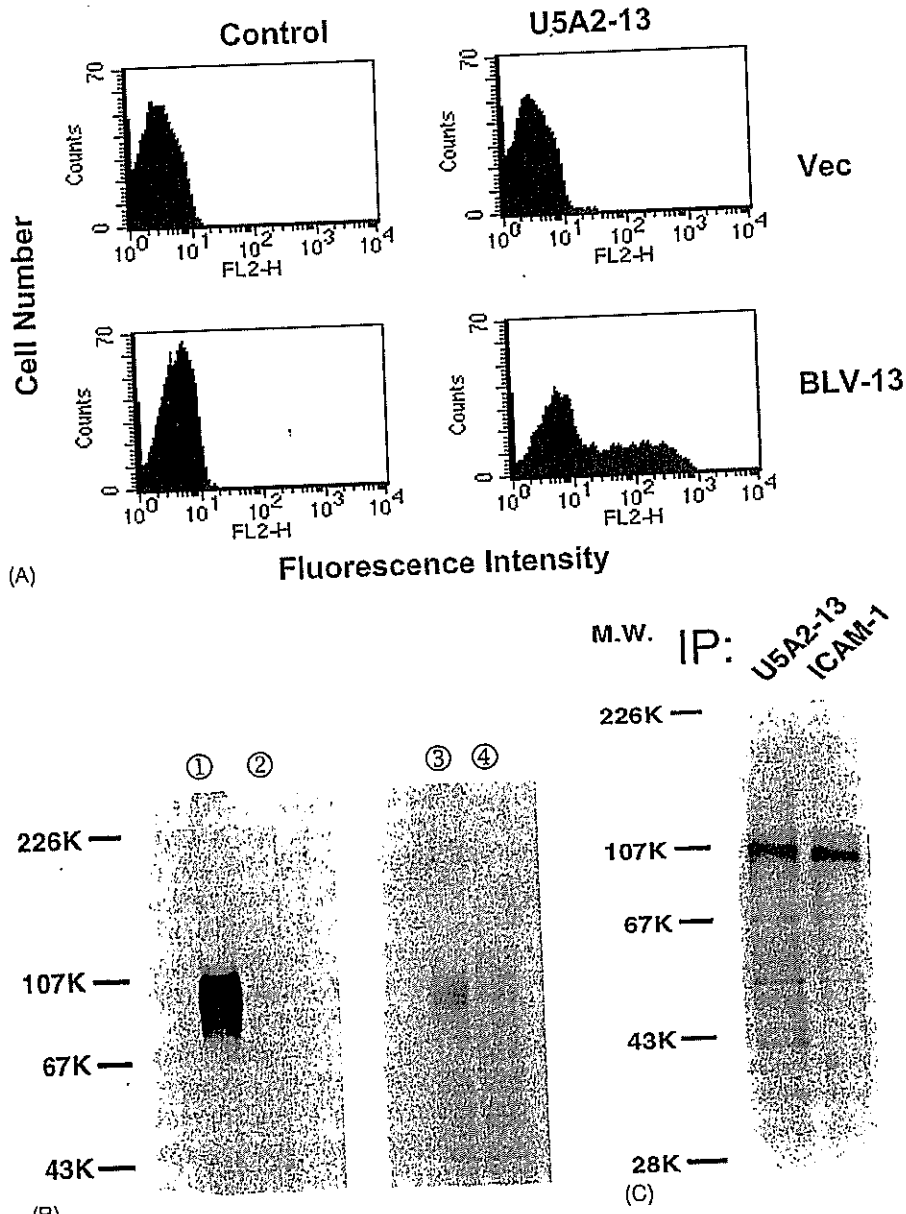

Fig. 1. Surface expression and biochemical analysis of U5A2-13-reactive molecules in COS-7 cells transfected with clone BLV-13 cDNA. (A) U5A2-13 mAb binds to COS-7 cells transfected with clone BLV-13 cDNA. COS-7 cells were transfected with pME18S vector alone (Vec) or with clone BLV-13 cDNA in pME18S (BLV-13), as indicated, right. Transfectants were stained with either PE-conjugated U5A2-13 mAb (U5A2-13) or PE-conjugated isotype-matched control Ab (Control) as indicated, above panel. Ab binding was detected by flow cytometry. (B) Western blotting of COS-7 cells transfected with clone BLV-13. Whole lysates of COS-7 cells transfected with clone BLV-13 were Western blotted. Lanes 1 and 2, transfected and control COS-7 cells detected with anti-ICAM-1 Ab, respectively; lanes 3 and 4, transfected and control COS-7 cells stained with anti-ICAM-1 Ab plus its blocking peptides, respectively. (C) Immunoprecipitation analysis of protein encoded by clone BLV-13 cDNA. Cells were labeled with biotin, then proteins were immunoprecipitated with U5A2-13 mAb and anti-ICAM-1 Ab. Immunoprecipitates were denatured with SDS sample buffer containing 2-ME and resolved in 7.5% SDS-PAGE gels and blotted. The blot was visualized using avidin-biotinylated horseradish peroxidase macromolecular complex and ECL® detection reagents.